doi:10.1038/nature11435

Supplementary Figures

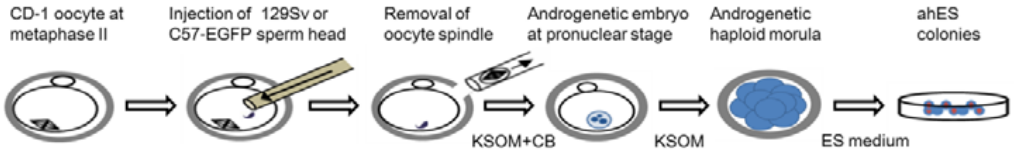

Figure S1. The scheme of androgenetic haploid embryonic stem (ahES) cells derivation.

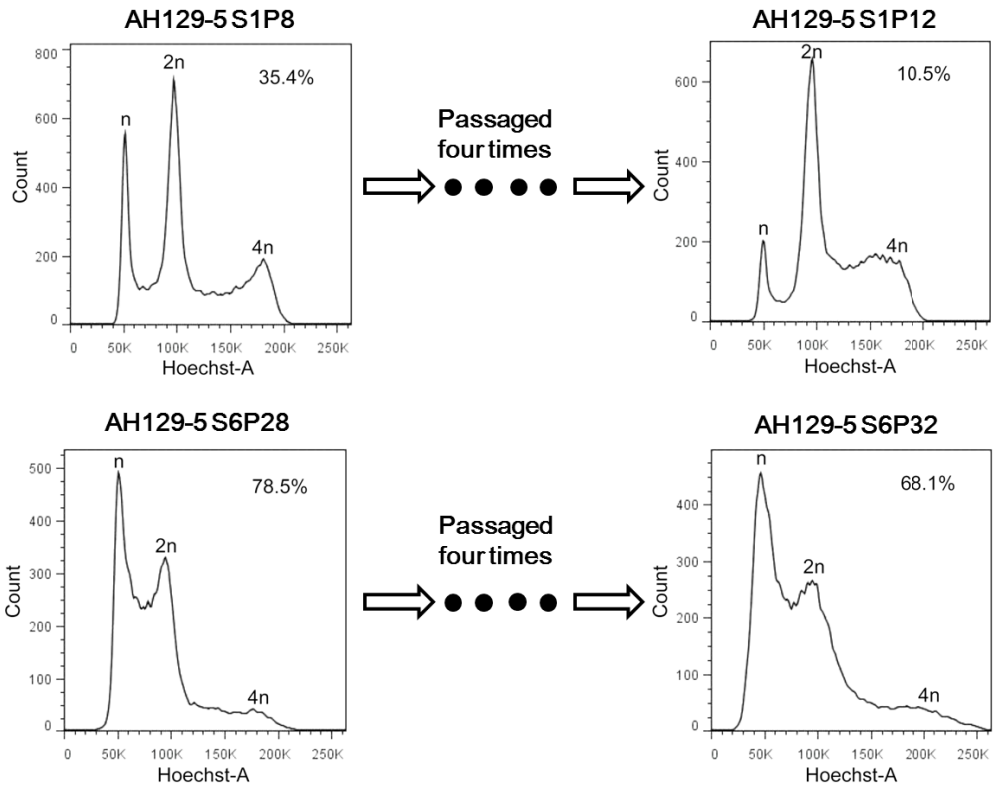

Figure S2. Karyotype analysis of haploid cells by FACS. The upper panels show the percentage of haploid cells in AH129-5 decreased rapidly in early passages (35.4% at P8 *vs.* 10.5% at P12) after being passaged four times without purification. After being sorted by FACS for six times, the percentage of haploid cells decreased slowly even without purification in late passages of ahES cells (78.5% at P28 *vs*. 68.1% at P32).

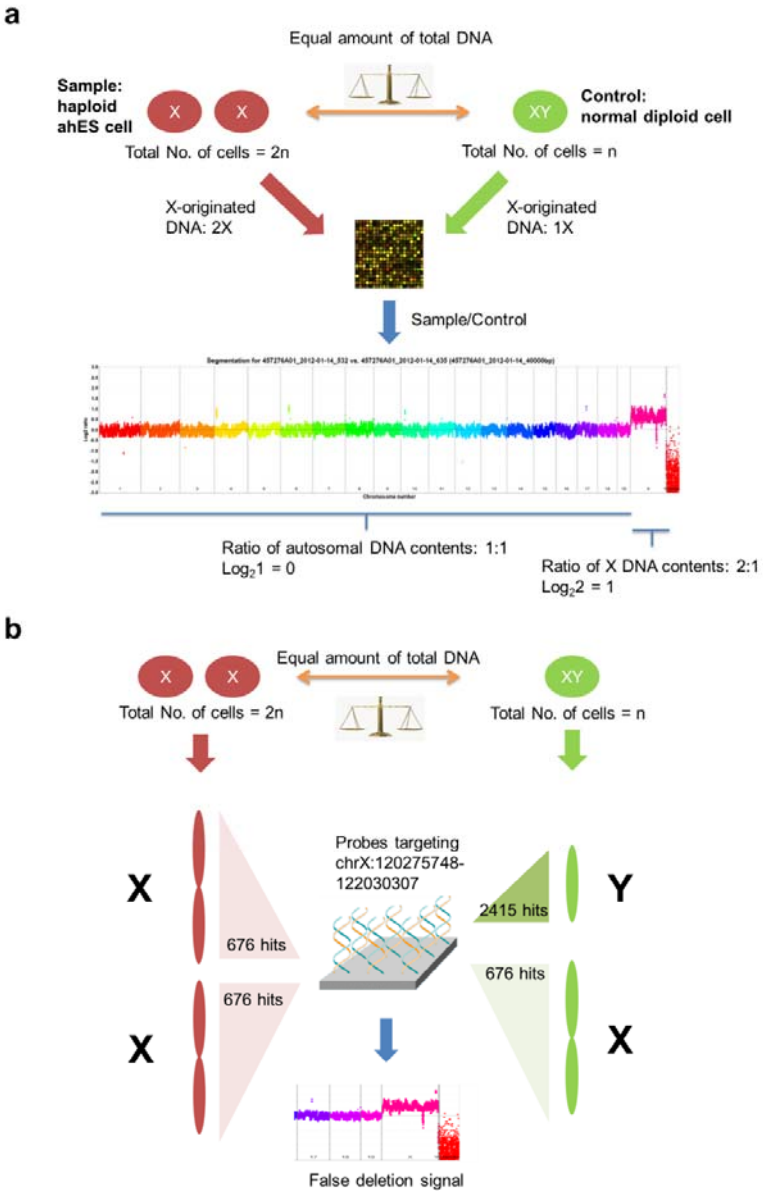

Figure S3. CGH analysis of X chromosome DNA content in ahES cells. a, Diagram illustrating the cause of high CGH array hybridization signals on the X chromosome of ahES cells. As the experiment was carried out using DNA from 129Sv male mice kidney cells as control, thus the content of X chromosome DNA should be twice in the ahES cells (one X chromosome every 20 chromosomes) than in the male control cells (one X chromosome every 40 chromosomes) when equal amount of genomic DNA was taken for hybridization in the CGH experiments. **b,** Diagram illustrating the reason for the regional deletion CGH array hybridization signals on the X chromosome of ahES cells. The regional deletion signals on the X chromosome in all ahES cell lines was an artifact due to the design problem of probes to the corresponding 1.75 Mb highly repetitive genomic region, as the 55 probes covering that region had 676 matches on the X chromosome and 2415 matches on the Y chromosome, resulting in stronger hybridization signals in this region of the wild type male control cells than of the ahES cells.

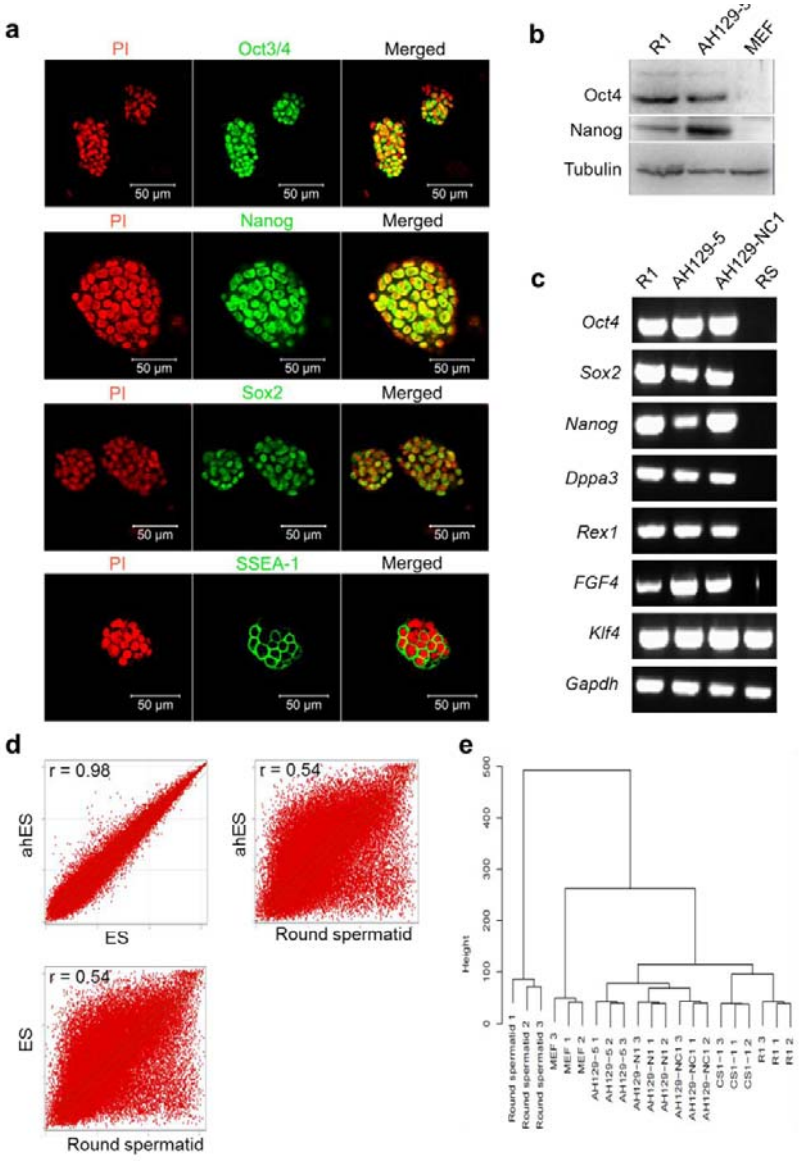

Figure S4. Characterization of ahES cells. a, Immunostaining of pluripotent markers Oct3/4 (green), Nanog (green), Sox2 (green) and SSEA-1 (green) in ahES cells. Propidium iodide (PI) is used to stain DNA (red). Scale bar, 50 μm. **b**, Western blot analysis of pluripotency markers Oct3/4 and Nanog in ahES cells. Tubulin is a loading control. **c**, RT-PCR analysis of pluripotent gene expression in two ahES cell lines (AH129-5 and AH129-NC1), one diploid ES cell line (R1) and round spermatids. *Gapdh* served as an internal control. **d,** Scatter plot of log2 transformed average gene expression profiles. Global gene expression of three ahES cell lines (AH129-5, AH129-NC1 and AH129-N1), two diploid ES lines (R1 ES and CS 1-1) and haploid round spermatid cells were obtained by microarray and analyzed by scatter plot (r is the Pearson correlation coefficient; red lines outline the twofold expression changes). **e,** Hierarchical clustering analysis of global gene expression patterns. Euclidean distance among cell lines is shown as the Y axis.

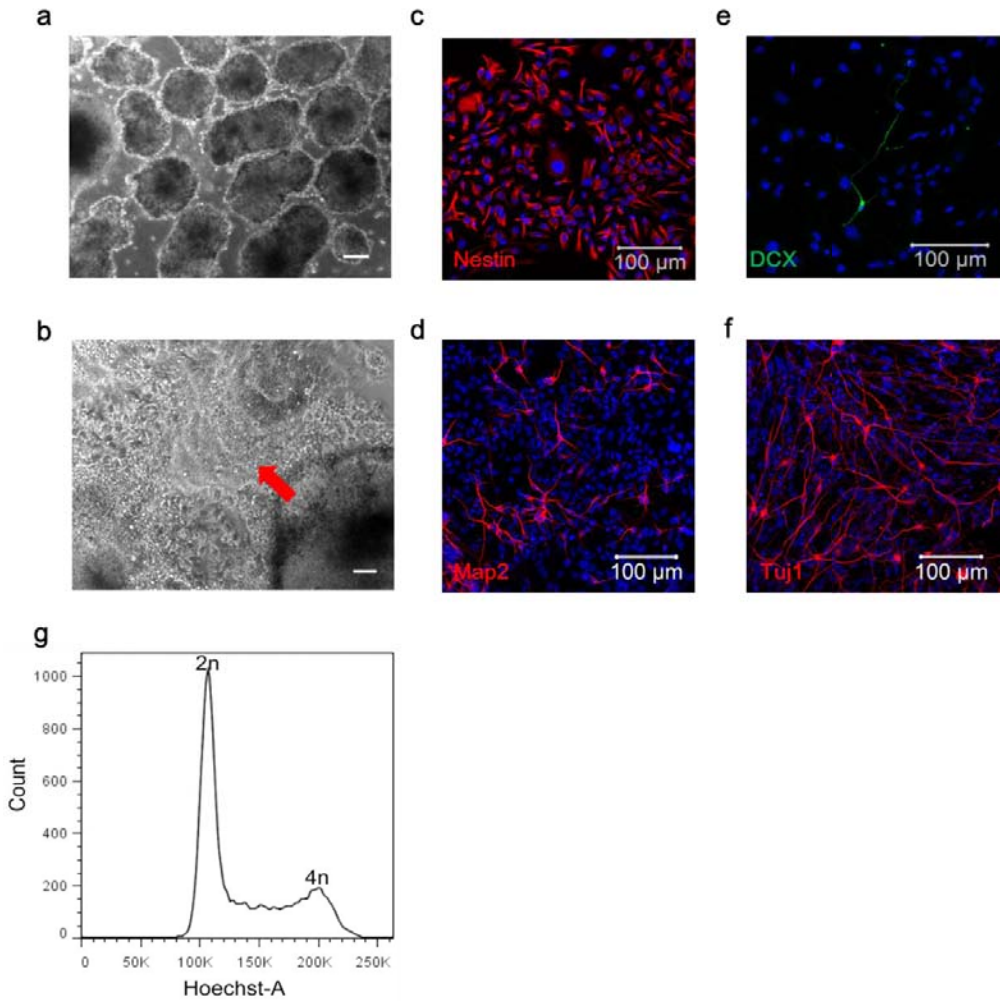

Figure S5. Directed differentiation of ahES cells into neural lineage. a, Bright field illumination of embryoid bodies (EBs) derived from ahES cells (cell line AH129-5). Scale bar, 100 μm. **b,** Typical rosette structure (red arrow) in haploid EBs. **c-f**, Immunostaining of specific neural markers (expressed in neural stem cells and neurons) in ahES cell differentiated cells (from AH129-5 cell line): **c,** Nestin. **d,** MAP2. **e,** Doublecortine (DCX). **f,** Tuj1. Scale bar, 100 μm. **g,** Flow cytometry analysis of DNA content of differentiated cells derived from ahES cells after ten days of neural differentiation.

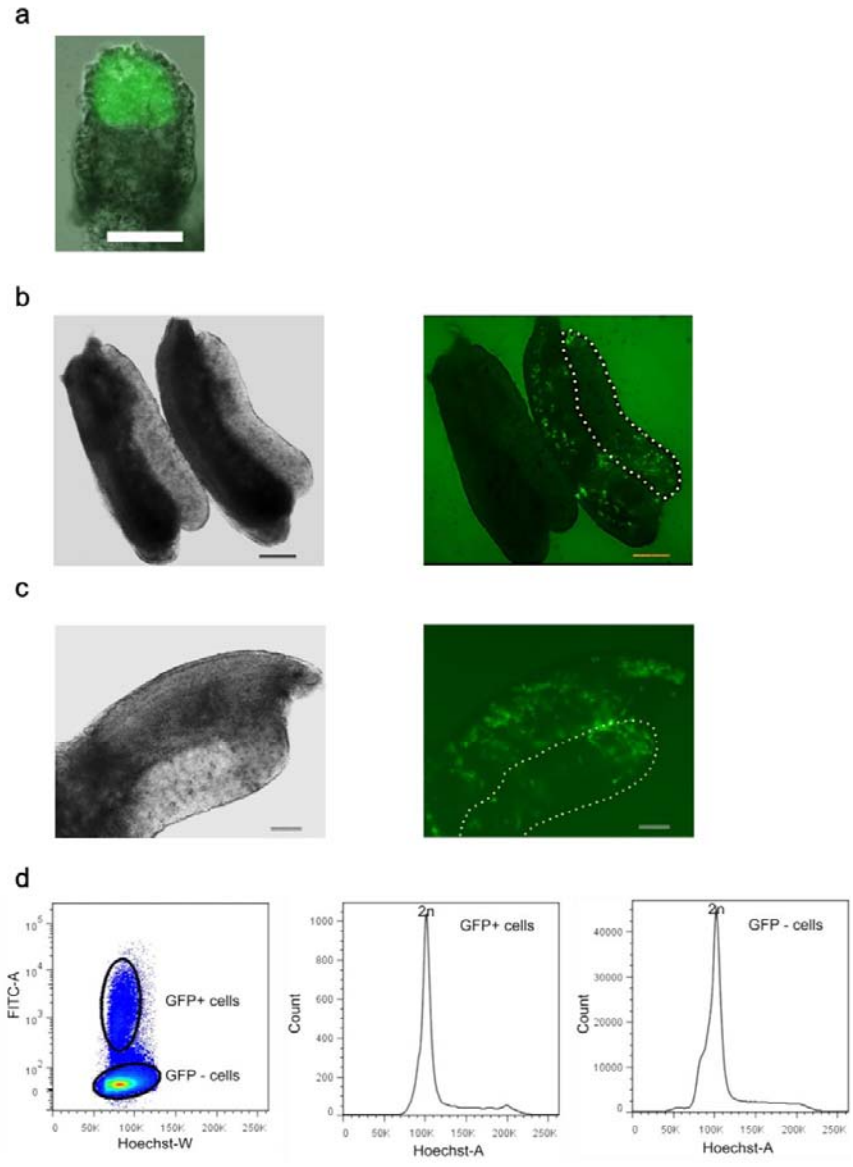

Figure S6. Flow cytometry analysis of DNA content of cells from ahES cells generated chimeric embryos. a, An E6.5 chimeric embryo with high contribution from ahES cells (AHGFP-4) that carrying chicken beta-actin eGFP gene. Bar = 100 µm. **b**, Fluorescence detection of the gonads (female) of E12.5 chimeric embryos, Gonads with (right) or without (left) eGFP expression are shown. Green fluorescence in genital ridge (marked in dashed frame) reflected contribution of the eGFP positive ahES cells (AHGFP-4). Bar = 200 µm. **c,** Florescence detection of gonads of E12.5 chimeric embryos in high magnification. Green fluorescence in genital ridge (marked in dashed frame) reflected contribution of the eGFP positive ahES cells (AHGFP-4). Bar =100 µm. **d,** Flow cytometry analysis of the DNA content of cells collected from the E12.5 chimeric embryos of Fig 2b. Both eGFP positive (from AHGFP-4) and negative (from CD-1 diploid embryo) cells are shown.

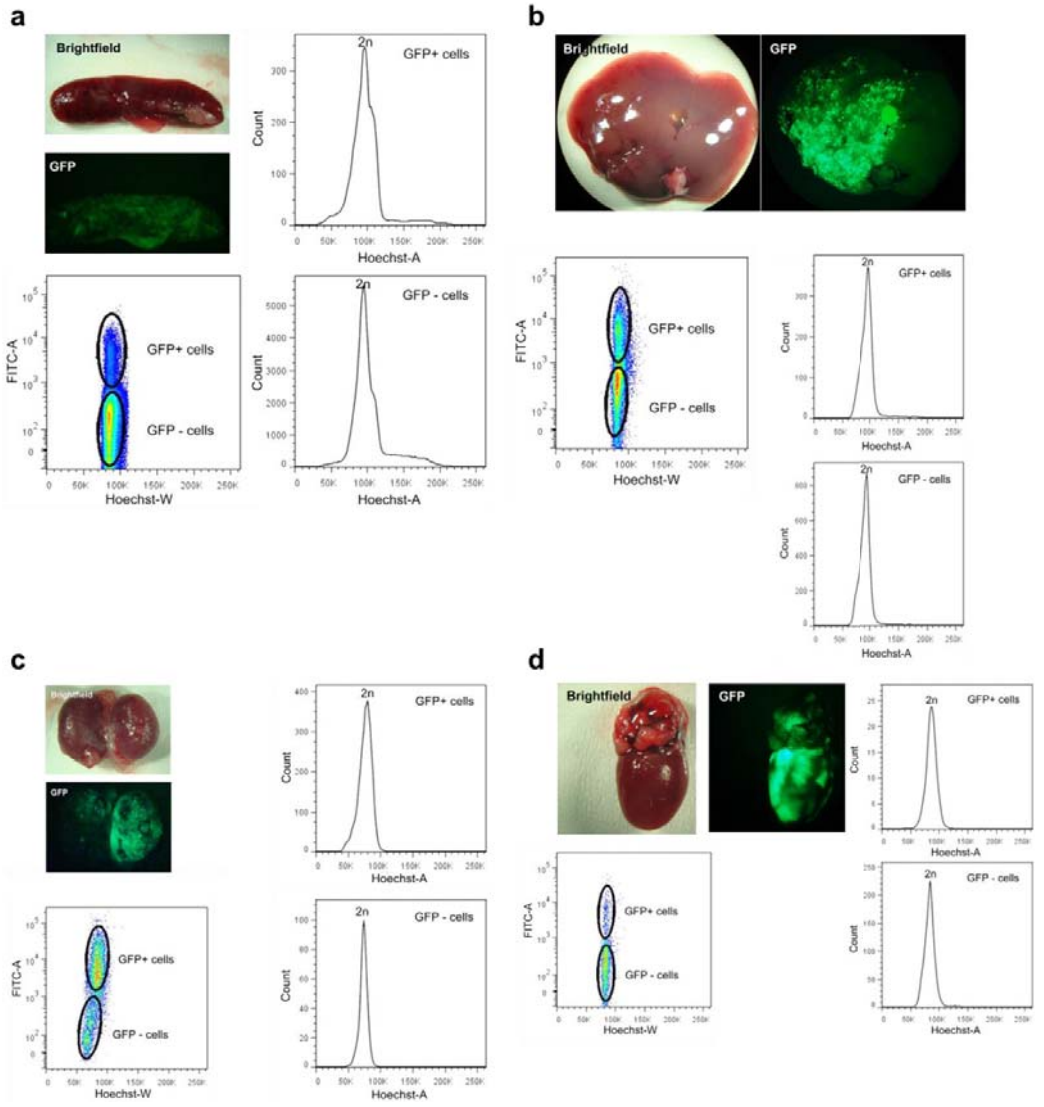

Figure S7. Flow cytometry analysis of DNA content of tissues dissected from adult chimeric mice. The chimeric mice were generated by injecting AHGFP-4 haploid cells into CD-1 wide type diploid blastocysts. **a,** Spleen. **b,** Liver. **c,** Kidney. **d,** Heart. Phase contrast and fluorescence images of these four tissues are shown. The contribution of AHGFP-4 cells is evidenced by the existing of eGFP positive cells in these organs. Flow cytometry analysis of the DNA content of eGFP positive and negative cells by FACS both showed completely diploid DNA content.

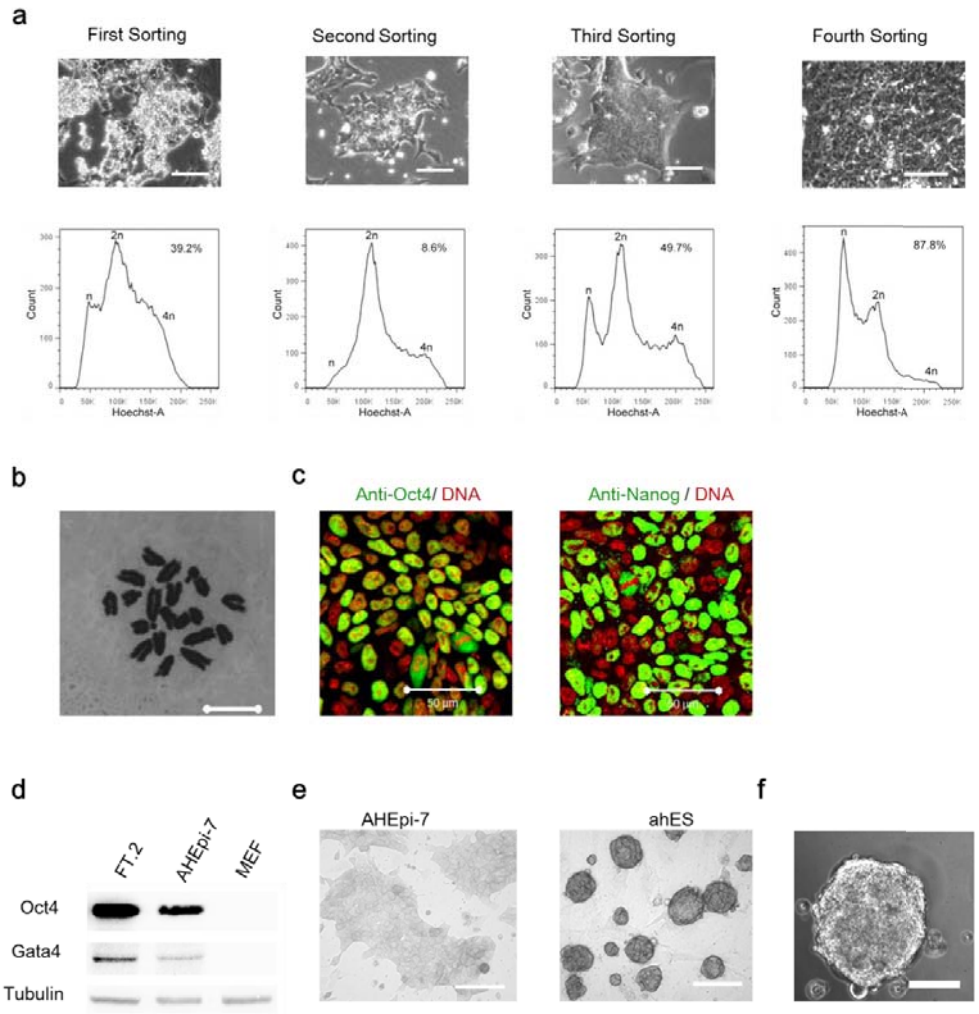

Figure S8. Characterization of haploid epiblast stem cell (EpiSC) like cells. a, Morphologies and haploid cell content of cells after the first four cycles of FACS sorting during the haploid EpiSC-like cell establishment process. **b,** Karyotype of an established haploid EpiSC-like cell line AHEpi-7. **c,** Expression of marker genes (green) in haploid EpiSC-like cells. Red is DNA. Scale bar, 50 μm. **d,** Western blot analysis of marker gene Oct4 and Gata4 expression in haploid EpiSC-like cell line AHEpi-7. Diploid EpiSCs derived from postimplantation embryo (FT.2[1]) are used as positive control and mouse embryonic fibroblasts (MEFs) are used as negative control. Tubulin is a loading control **e,** Alkaline phosphatase (AP) staining of the haploid EpiSC-like cells (EpiAH-7) and ahES cells (AH129-5). Bar = 100 μm. **f,** Day 4 embryoid body formation from the haploid EpiSC-like cells (AHEpi-7). Bar = 50 μm.

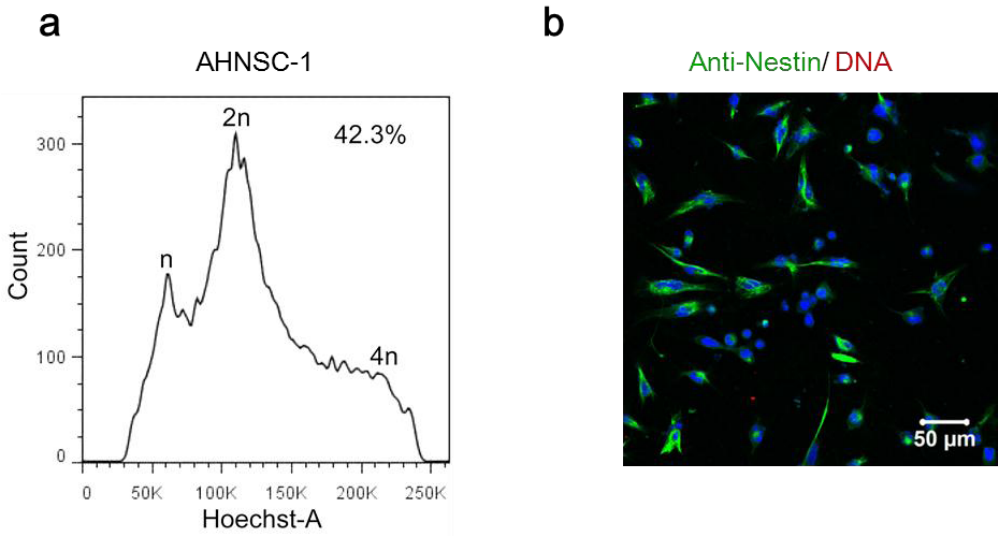

Figure S9. Flow cytometric analysis of DNA content of neural progenitor cells. a, Flow cytometric analysis of DNA content in AHEpi-7 derived early neural progenitors. A total of 42.3% of the AHEpi-7 cell derivatives are haploid. **b**, Nestin (green) is expressed in haploid neural progenitor cells cultured two days after FASC-purification. Hoechst is used to stain DNA (blue). Scale bar, 50 µm.

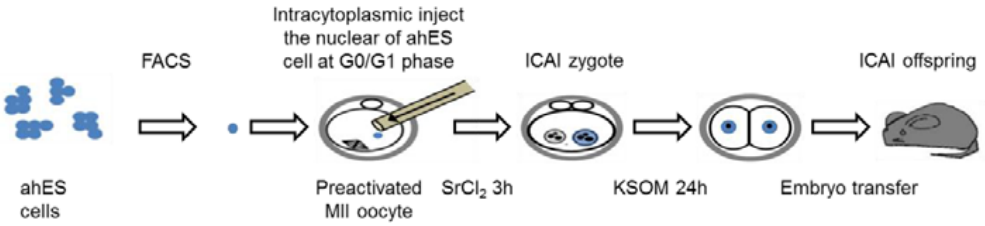

Figure S10. Schematic overview of the ICAI procedure.

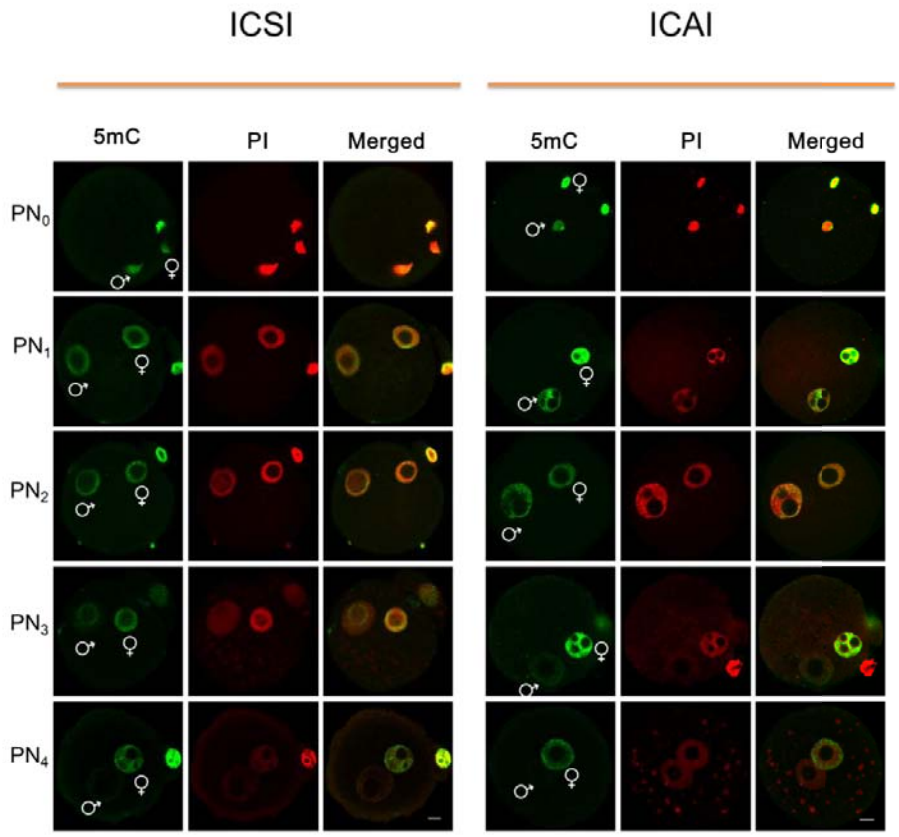

Figure S11. 5mC and DNA immunostaining of embryos produced by ICSI and ICAI. Embryos produced by ICSI (left) and ICAI (right) are immunostained by 5mC (green) and PI (red) to trace the "paternal" pseudo-pronucleus formation (♂ marked) and dynamic DNA demethylation of the "paternal" pseudo-pronucleus. Bar = 10 μm.

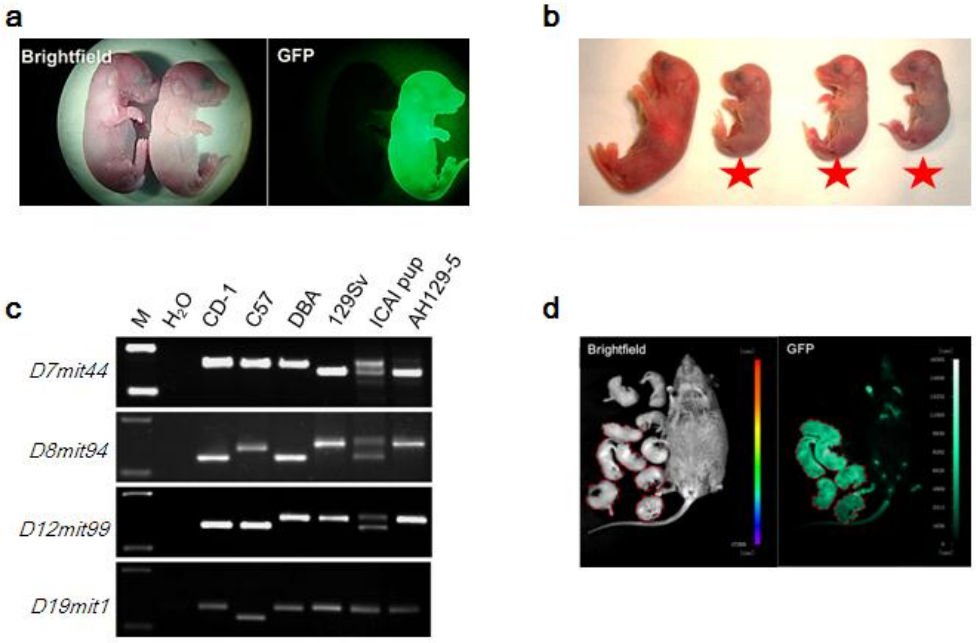

Figure S12. Generation and identification of the ICAI offspring. a, Full term ICAI pups produced by ahES cell lines AH129-5 (left, eGFP negative) and AHGFP-4 (right, eGFP positive). **b,** Comparison of body size of several ICAI offspring. The most left pup survived to adulthood, the others indicated by stars were of smaller body size and died within 30 min after birth. **c,** SSLP analysis of obtained full-term ICAI pups from cell line AH129-5. Four DNA markers from different chromosomes show that the ICAI pups are derived from two genetic backgrounds, the CD1 strain (oocyte origin) and the 129Sv strain (ahES cells origin). **d,** Fluorescence detection of an AHGFP-4 ICAI offspring (female, eGFP positive) and its offspring under NightOWL II. The eGFP-pups are outlined by dotted lines.

a

Cell line	Cell type	No. of G418 resistant colonies from $5x10^6$ electroporated cells	No. of random picked colonies	No. of colonies contained haploid cells
R1	Diploid ES cells	196	ND	ND
AHGFP-4	ahES cells	187	12	6

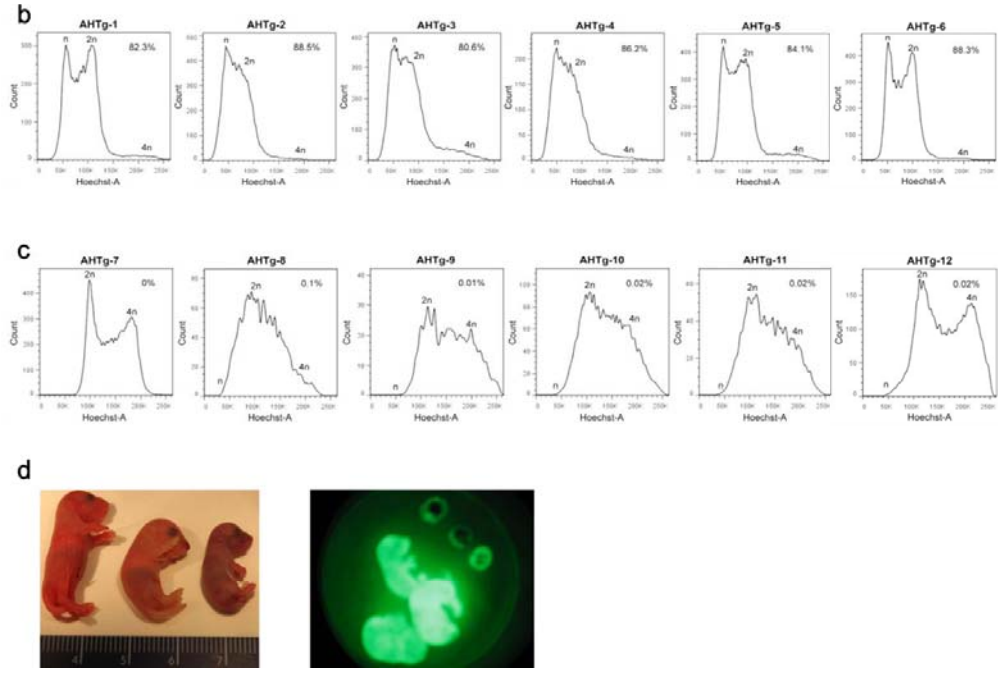

Figure S13. Application of ahES cells in transgenic studies. a, The transgenic efficiency of a neomycin resistant gene (*neo*^{r}) in a normal ES cell line R1 and an ahES cell line AHGFP-4. The transgene was introduced to cells by electroporation. The picked G418 resistant colonies were expanded for 1-2 passages then purified by flow cytometric analysis. **b**, Six *neo*^{r}-transgenic sublines (AHTg-1 to 6, from AHGFP-4) maintained high percentage of haploid cells. **c,** The other 6 sublines (AHTg-7 to 12) were almost completely diploidized. **d,** Pictures of the two alive pups (left and middle) and one early-dead pup (right) under bright filed (left) and fluorescence microscope (right).

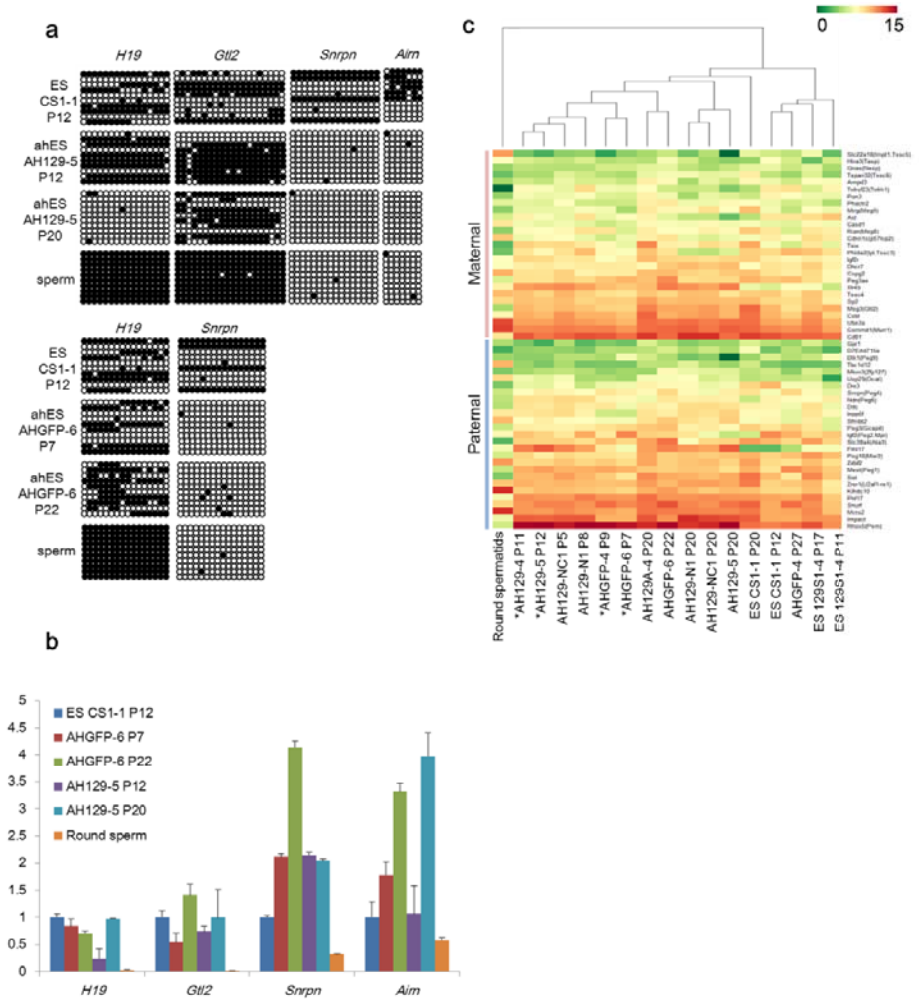

Figure S14. Methylation and expression analysis of the haploid ahES cell lines and ahES cell derived animals. a, Bisulfite genomic sequencing analysis of DMRs of imprinted genes *H19*, *Snrpn*, *Gtl2* and *Airn* in ES cells (CS1-1, P12), ahES cells (AH129-5, P12 and P20; AHGFP-6, P7 and P22) and round spermatids. Filled circles represent methylated CpG sites. Open circles represent unmethylated CpG sites. **b,** Histogram of expression levels of paternally imprinted genes *H19*, *Gtl2* and maternally imprinted genes *Snrpn* and *Airn* in ahES cell lines (AH129-5, P12 and P20; AHGFP-6, P7 and P22) and round spermatids as compared to a normal diploid ES cell line (CS 1-1, P12). The expression of endogenous *Gapdh* of each cell line is used as control. Error bars represent standard deviation (n=3). **c,** Clustering analysis of the expression of imprinted genes among round spermatids (RS), normal diploid ES cell lines (129S1-4, P11 and P17; CS 1-1, P12 and P20), and multiple ahES cell lines including both early passage and late passage of ICAI reproduction-competent ahES cell lines (labeled with star, AH129-4, P11 and P20; AH129-5, P12 and P20; AHGFP-4, P9 and P27; AHGFP-6, P7 and P22) and ICAI reproduction-incompetent ahES cell lines (AH129-N1, P8 and P20; AH129-NC1, P5 and P20).

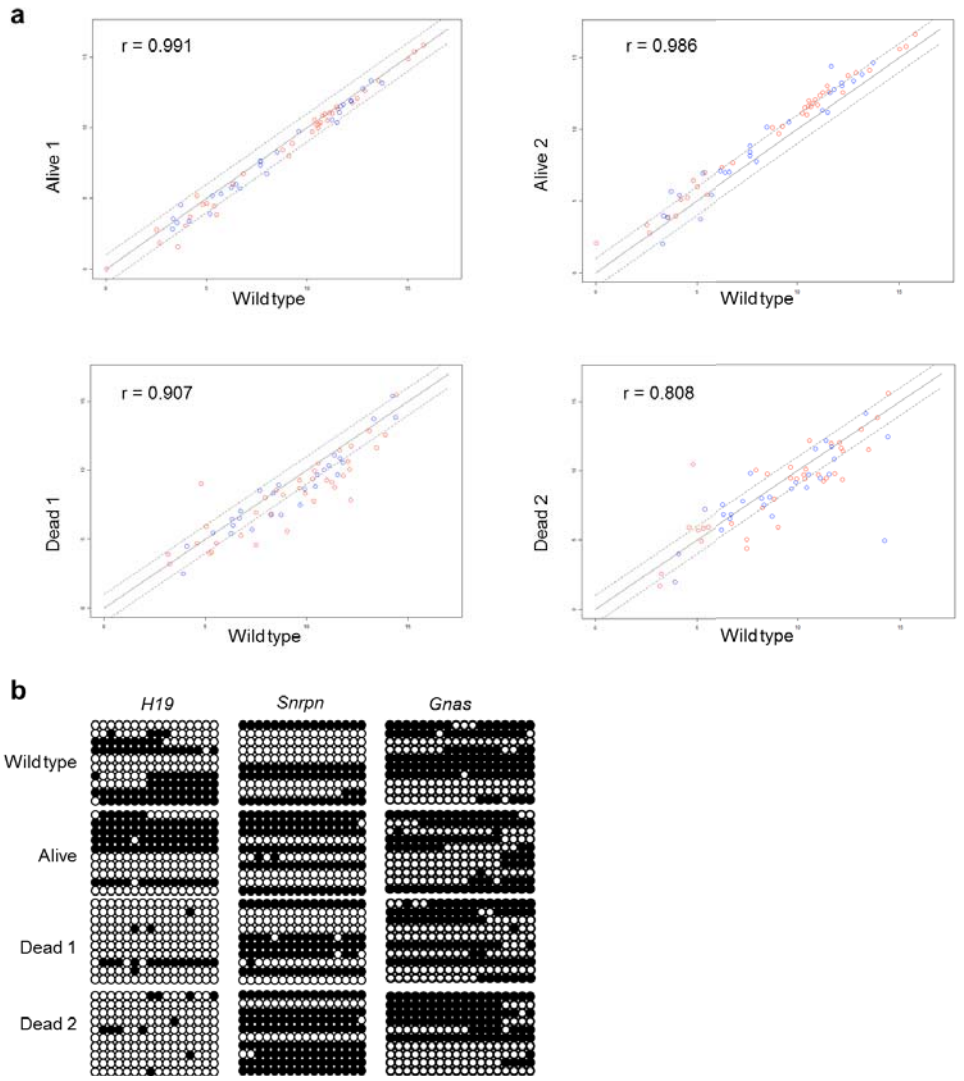

Figure S15. Comparison of imprinted genes among control mice, alive and early-dead (died within 30 min after birth) ahES cell derived ICAI mice. a, Expression comparison of imprinted genes among control mice, alive and early-dead ahES cell derived ICAI mice. RNAs extracted from kidney of wild type mice, alive and early-dead ahES cell derived ICAI mice are used in the experiment. The log2 transformed comparison results of real-time PCR data of 54 imprinted genes are presented as scatter lots. The expression profile of imprinted genes in alive ICAI mice are highly similar to that of the controls (upper panels), whereas the early-dead mice show more variations from the control. b, Bisulphite genomic sequencing analysis of DMRs of imprinted genes *H19*, *Snrpn* and *Gnas* in a wild type control, an alive ICAI-produced pup and two stillborn mice.

Supplementary Tables.

Table S1. *In vitro* development of androgenetic haploid embryos.

Group	Oocyte	Sperm	Reconstructed	PN	2-cell (%)	4-cell (%)	Morula (%)
1	B6D2F1	129Sv	106	104	98 (94.2)	44 (41.5)	24 (22.6)
2	B6D2F1	129Sv	381	377	323 (84.8)	139 (36.5)	69 (18.1)
3	B6D2F1	B6D2F1	283	281	239 (84.5)	145 (51.2)	67 (23.7)
4	B6D2F1	129Sv	224	222	206 (92.0)	97 (43.3)	45 (20.1)
5	B6D2F1	Beta-actin -eGFP	175	172	156 (89.1)	97 (55.4)	42 (24.0)
6	B6D2F1	Oct4-eGFP	72	70	61 (84.7)	40 (55.6)	15 (20.8)

* The *in vitro* development efficiencies (shown as %) are calculated based on the total reconstructed embryos.

Table S2. Establishment efficiency of ahES cell lines by different methods.

Group	Derivation medium	No. of morulas	No. of haploid ES cell lines (Derivation efficiency)	Names of haploid ES cell lines
1	N2B27+2i+Lif	24	3 (12.5%)	AH129-N1, AH129-N2, AH129-N3
2	N2B27+2i+Lif+ P53i[1)]	69	7 (10.1%)	AH129-1, AH129-2, AH129-3, **AH129-4[3)]**, **AH129-5[3)]**, AH129-6, AH129-7
3	N2B27+2i+Lif+ P53i	67	5 (7.5%)	AHF1-1, AHF1-2, AHF1-3, AHF1-4, AHF1-5
4	N2B27+2i+Lif+ P53i+3c[2)]	45	2 (4.4%)	AH129-NC1, AH129-NC2
5a	N2B27+2i+Lif+ P53i+5%KSR	42	8 (19.0%)	AHGFP-1, AHGFP-2, AHGFP-3, **AHGFP-4[3)]**, AHGFP-5, **AHGFP-6[3)]**, AHGFP-7, AHGFP-8
5b	N2B27+2i+Lif+ P53i+5%KSR	15	2 (13.3%)	AHOG-1, AHOG-2
5c	N2B27+2i+Lif	/	/	**AHTg-1[3)]**, AHTg-2, **AHTg-3[3)]**, AHTg-4, AHTg-5, AHTg-6, AHTg-7, AHTg-8, AHTg-9, AHTg-10, AHTg-11, AHTg-12,

1) P53i: Piffithrin-α, an inhibitor of P53.
2) 3c: antioxidant combination (Vc, α-lipoic, α-tocopherol).
3) Cell lines capable of producing viable progenies via ICAI are shown in bold.
4) The derivation efficiency is calculated based on the total implanted morulas.

Table S3. List of CNV regions detected by the CGH array.

Region	Length	AH129-5	AH129-NC1	AH129-N1	Overlap genes
chr1:117826831-117923865	97034	-1.08	-0.96	-1.03	Cntnap5a
chr3:25419265-25452686	33421	-1.37	-1.38	-1.53	Nlgn1
chr4:10734684-12021734	1287050	0.87	0.00	0.00	2610301B20Rik, Plekhf2, 2310030N02Rik, Mir684-2,Trp53inp1, Ccne2,Ints8, Dpy19l4,Esrp1, 1110037F02Rik, Rad54b,Gem, Cdh17,Pdp1,Tmem67
chr4:12022544-12533707	511163	0.67	0.00	0.00	Rbm12b,Fam92a
chr6:39076106-39315435	239329	0.96	0.00	0.00	Jhdm1d,Slc37a3
chr6:39315435-39497694	182259	0.96	0.00	0.26	Slc37a3,Rab19,Mkrn1, Dennd2a
chr6:39497694-39628909	131215	0.96	0.00	0.00	Dennd2a,Adck2, Ndufb2,Braf
chr6:70073072-70090963	17891	0.00	0.00	-0.52	none
chr6:70094644-70113132	18488	0.00	0.00	-2.26	none
chr6:70116932-70244308	127376	0.00	0.00	-1.11	none
chr6:70247628-70277006	29378	0.00	0.00	-1.48	none
chr6:70278401-70332885	54484	0.00	0.00	-0.40	none
chr6:70335957-70353025	17068	0.00	0.00	-0.80	none
chr10:19953534-20223311	269777	0.83	0.00	0.00	Mtap7,Bclaf1,Fam54a, Pde7b
chr12:35569232-35593102	23870	-1.91	0.00	0.00	none
chr12:96146363-96178064	31701	0.00	-1.98	0.00	none
chr17:42974884-43090635	115751	0.98	0.00	0.00	Cd2ap
chrX:120275748-120290676	14928	0.00	-0.62	-0.64	none
chrX:120290676-120337179	46503	-0.77	-0.62	-0.64	none
chrX:120337179-120342114	4935	0.00	-0.62	-0.64	none
chrX:120342114-120360725	18611	-0.28	-0.62	-0.64	none
chrX:120730365-120787132	56767	-0.67	-0.76	-0.81	none
chrX:121999026-122002467	3441	0.50	0.44	-1.02	none
chrX:122002467-122003805	1338	0.00	0.00	-1.02	none
chrX:122003805-122022914	19109	0.00	-0.70	-1.02	none
chrX:122022914-122026184	3270	0.00	-0.70	0.00	none
chrX:122026184-122030307	4123	0.00	-0.70	0.51	none
chrX:166498497-166525781	27284	0.41	-1.96	0.42	none
chrX:166578982-166630742	51760	0.41	-3.23	0.42	none
chrX:166635572-166648536	12964	0.41	-1.01	0.42	none

Table S4. Developmental analysis of haploid G0/G1 stage ahES cells by diploid blastocysts injection.

Cell line	No. of injected blastocysts	No. of arrested <10.5d	No. of eGFP$^+$ E6.5	No. of germline contribution of E12.5	No. of newborn pups	No. of chimeric pups	Coat color chimerism (%)
*AHGFP-4	46	16	6/17	/	/	/	/
**AHGFP-4	88	24	/	4/23	/	/	/
***AHOG-2	81	27	/	6/11	/	/	/
AH129-N1	82	/	/	/	7	1	10%
AH129-5	40	/	/	/	3	2	20%
AHGFP-4	98	/	/	/	3	2	25%

* Chimeric embryos dissected at E6.5, six of seventeen E6.5 chimeric embryos contained eGFP positive cells.

** Chimeric embryos dissected at E12.5, four of twenty-three E12.5 chimeric embryos contained eGFP positive cells within the dissected gonads.

*** Chimeric embryos dissected at E12.5, six of eleven E12.5 chimeric embryos contained Oct4-eGFP positive cells within the dissected gonads.

Table S5. Developmental efficiency of ICAI embryos from gene modified ahES cells (New data obtained during the manuscript revision process).

Donor cells	No. of injected oocytes	No. of cleavage	No. of transferred embryos	No. of implantation (%ET)	No. of full term pups (%ET)	No. of survived (%ET)
AHTg-1	453	330 (72.8)	330	64*	20 (6.1)	5 (1.5)
AHTg-2	164	115 (70.1)	115	43 (37.4)	1 (0.9)	0
AHTg-3	316	247 (78.2)	247	56 (22.7)	2 (0.8)	1 (0.4)

*The implantation count is incomplete and does not include those in the surrogate mothers with nature labor of AHTg-1 produced mice.

Table S6. Primers used in PCR analysis.

Category	Gene	Primers (5'→3')
RT-PCR	Oct4	Forward: GGCTTCAGACTTCGCCTCC Reverse: AACCTGAGGTCCACAGTATGC
	Nanog	Forward: AGGATGAAGTGCAAGCGGTG Reverse: GGGATAGCTGCAATGGATGC
	Sox2	Forward: TGCCTCTTTAAGACTAGGGC Reverse: TCTGGCGGAGAATAGTTGG
	Dppa3	Forward: GGGAAGTTCAAAGCGCCTTTC Reverse: ACTCATTTCCTTCGAGCCTTTTT
	Rex1	Forward: TTAGCCCCGAGACTGAGGAAG Reverse: CTTGCGTGACCTCTCTCTTCT
	Fgf4	Forward: TGGGCCTCAAAAGGCTTCG Reverse: CGTCGGTAAAGAAAGGCACAC
	Klf4	Forward: CCATCGGACCTACTTATCTGC Reverse: AAAACCTCAAACCAAAACCC
	Gapdh	Forward: AGGTCGGTGTGAACGGATTTG Reverse: TGTAGACCATGTAGTTGAGGTCA
	H19	Forward: TACCCCGGGATGACTTCATC Reverse: TATCTCCGGGACTCCAAACC
	Snrpn	Forward: GTGGGGAGAACTTGGTTTCAAT Reverse: TGCAGCGCCAGCAAGA
	Gtl2	Forward: CCATTTGCTGTTGTGCTCAGGT Reverse: TGCAACGTGTTGTGCGTGAAG
	Actin	Forward: AGGCACCAAGGTGTGATGGT Reverse: GGTCTCAAACATGATCTGGG
	T (Brachyury)	Forward: GCTTCAAGGAGCTAACTAACGAG Reverse: CGTCACGAAGTCCAGCAAGA
	FGF5	Forward: TGTGTCTCAGGGGATTGTAGG Reverse: AGCTGTTTTCTTGGAATCTCTCC
	Cer1	Forward: GGATGTGGAAAGCGATCATGT Reverse: ATGCCAGAACCTCTTGGCTTC
	Sox17	Forward: CCAAAGCGGAGTCTCGCAT Reverse: GCCTAGCATCTTGCTTAGCTC
Sex determination	Zfy	Forward: AAGATAAGCTTACATAATCACATGGA Reverse: CCTATGAAATCCTTTGCTGCACATGT
	Phex	Forward: TGAGCAGGTAGGCAGTC Reverse: GAGGTAAGGCAGGGTC
DMR bisulphite sequencing	H19	Forward: TATGAGTATTTAGGAGGTATAAGAATT Reverse: TTTTATCAAAAACTAACATAAACCCCT 1st PCR round

		Forward: TGTAAGGAGATTATGTTTTATTTTTGG Reverse: CCCTAACCTCATAAAACCCATAACTAT 2nd PCR round
	Gnas	Forward: GTTTATGGGTCGGTTTTTTGAAGAGGTT Reverse: TCTACCCTATCCCAACTCTTACCTACT 1st PCR round
		Forward: GGGTTGTTTTAGGTGGTTGGTATTAG Reverse: ACTCTTACCTACTCGAACACCTC 2nd PCR round
	Snrpn	Forward: TATGTAATATGATATAGTTTAGAAATTAGT Reverse: AATAAACCCAAATCTAAAATATTTTAATCA 1st PCR round
		Forward: AATTTGTGTGATGTTTGTAATTATTTGG Reverse: ATAAAAATACACTTTCACTACTACTAAAAT 2nd PCR round
	Gtl2	Forward: TGGTCTGGGGGCAGCCCCTTACTGCAG Reverse: GAGGGGTACAGATGAATTGATTGACAGGTCACAAG 1st PCR round
		Forward: ACCCTTAAAGATGGCTGATGTGGGCTC Reverse: GAGGGGTACAGATGAATTGATTGACAGGTCACAAG 2nd PCR round
	Airn	Forward: GTTAGTGGGGTATTTTTATTTGTATGG Reverse: AAAATATCCTAAAAATACAAACTACAC 1st PCR round
		Forward: GTTAGTGGGGTATTTTTATTTGTATGG Reverse: AGTGTGGTATTTTTATGTATAGTTAGG 2nd PCR round

Reference

1 Maruotti, J. *et al.* Nuclear transfer-derived epiblast stem cells are transcriptionally and epigenetically distinguishable from their fertilized-derived counterparts. ***Stem Cells*** 28, 743-752, doi:10.1002/stem.400 (2010).